



## OPEN ACCESS

## EDITED BY

Ana Claudia A. Melo,  
Federal University of Rio de Janeiro, Brazil

## REVIEWED BY

Xue-Qing Yang,  
Shenyang Agricultural University, China  
Nathália F. Brito,  
National Cancer Institute (INCA), Brazil

## \*CORRESPONDENCE

Tao Zhang,  
✉ cauzht@163.com  
Zhanlin Gao,  
✉ zbs308@163.com

RECEIVED 04 August 2024

ACCEPTED 09 December 2024

PUBLISHED 06 January 2025

## CITATION

Guo J, Liu P, Zhang X, An J, Li Y, Zhang T and Gao Z (2025) Characterization of the ligand-binding properties of odorant-binding protein 38 from *Riptortus pedestris* when interacting with soybean volatiles.  
*Front. Physiol.* 15:1475489.  
doi: 10.3389/fphys.2024.1475489

## COPYRIGHT

© 2025 Guo, Liu, Zhang, An, Li, Zhang and Gao. This is an open-access article distributed under the terms of the [Creative Commons Attribution License \(CC BY\)](https://creativecommons.org/licenses/by/4.0/). The use, distribution or reproduction in other forums is permitted, provided the original author(s) and the copyright owner(s) are credited and that the original publication in this journal is cited, in accordance with accepted academic practice. No use, distribution or reproduction is permitted which does not comply with these terms.

# Characterization of the ligand-binding properties of odorant-binding protein 38 from *Riptortus pedestris* when interacting with soybean volatiles

Jianglong Guo, Panjing Liu, Xiaofang Zhang, Jingjie An, Yaofa Li, Tao Zhang\* and Zhanlin Gao\*

Plant Protection Institute, Hebei Academy of Agriculture and Forestry Sciences, Key Laboratory of Integrated Pest Management on Crops in Northern Region of North China, Ministry of Agriculture and Rural Affairs, IPM Innovation Center of Hebei Province, International Science and Technology Joint Research Center on IPM of Hebei Province, Baoding, China

**Background:** *Riptortus pedestris* (Fabricius) (Hemiptera: Alydidae) is a major soybean pest throughout East Asia that relies on its advanced olfactory system for the perception of plant-derived volatile compounds and aggregation pheromones for conspecific and host plant localization. Odorant binding proteins (OBPs) facilitate the transport of odorant compounds across the sensillum lymph within the insect olfactory system, enabling their interaction with odorant receptors (ORs).

**Methods:** Real-time quantitative PCR (qRT-PCR) analyses, fluorescence-based competitive binding assays, and molecular docking analyses were applied to assess the expression and ligand-binding properties of OBP38 from *R. pedestris*.

**Results:** The qRT-PCR analyses revealed high levels of *RpedOBP38* expression in the antennae without any apparent sex bias, and it was also highly expressed in the adult stage. Recombinant *RpedOBP38* was prepared by expressing it in *E. coli* BL21 (DE3) followed by its purification with a Ni-chelating affinity column. *RpedOBP38* was found to bind most strongly to trans-2-decenal ( $K_i = 7.440$ ) and trans-2-nonenal ( $K_i = 10.973$ ), followed by  $\beta$ -pinene, (+) -4-terpineol, carvacrol, methyl salicylate, and (-)-carvone. The 3D structure of *RpedOBP38* contains six  $\alpha$ -helices and three interlocked disulfide bridges comprising a stable hydrophobic binding pocket. In a final series of molecular docking analyses, several polar (e.g., His 94, Glu97) and nonpolar (e.g., Leu29, Ile59) residues were found to be involved in *RpedOBP38*-ligand binding.

**Conclusion:** These data support a role for *RpedOBP38* in the perception of volatiles derived from host plants, providing important insight into the mechanisms that govern olfactory recognition in *R. pedestris*, thereby informing the development of ecologically friendly approaches to managing *R. pedestris* infestations.

## KEYWORDS

*Riptortus pedestris*, OBPs, soybean volatiles, fluorescence competitive binding, molecular docking

## 1 Introduction

The ability of insects to perceive pheromones, host-derived odorants, and the wide array of other peripheral chemical signals present in their surrounding environment is dependent on a complex olfactory system that ultimately shapes key physiological processes such as foraging, mating, and oviposition (Martin et al., 2011; Leal, 2013). The ability to accurately recognize and decipher these signals is thus vital for the ability of insects to survive and reproduce. Hydrophobic chemicals need to successfully penetrate the olfactory sensilla and the hydrophilic sensillum lymph in order to access the odorant receptors (ORs) present on sensory neuron surfaces, thereby triggering downstream signal transduction (Li et al., 2015; Zhou et al., 2022). To facilitate this process, specialized supporting cells produce odorant-binding proteins (OBPs), which are secreted into the olfactory sensillum lymph and play a vital role in the process of insect odorant reception (Leal, 2013; Paula et al., 2018). OBPs can selectively bind, solubilize, and transport odorant molecules as they diffuse into the sensillum lymph, thereby enabling the activation of ORs and associated downstream signaling pathways (Leal, 2013; Liu et al., 2023). Given the importance of OBPs during this initial stage of odorant reception, they hold great promise as molecular targets for pest control efforts and the development of superior integrated pest management (IPM) strategies (Zhou et al., 2010; Venthur and Zhou, 2018).

The OBPs produced by insects are low-molecular-weight (12–20 kDa) proteins approximately 100–200 amino acids in length that are water soluble and typically feature a ~20 amino acid N-terminal signal peptide sequence (Ahmed et al., 2017; Li J. B. et al., 2022; Zeng et al., 2019). The 3D structures of classical OBPs are stabilized by three disulfide bridges formed by six conserved cysteine residues (Leal et al., 1999; Scaloni et al., 1999; Pelosi et al., 2014). The patterns of conserved cysteines have also been used to define four other classes of OBPs, including “Dimer” OBPs with two typical cysteines, “Minus-C” OBPs that lack 1–2 cysteines, “Plus-C” OBPs with 2–3 extra cysteines, and “Atypical” OBPs with a long, atypical C-terminal domain (Zhou et al., 2010; Spinelli et al., 2012; Manoharan et al., 2013; Venthur et al., 2014; Zeng et al., 2019). Identified in 1981, the first characterized OBP in insects was found to be exclusively expressed in *Antberaea polyphemus* antennae, enabling male moths to detect a particular sex pheromone (*trans*-6, *cis*-11-hexadecadienyl acetate) such that they were able to locate conspecific females to engage in mating (Vogt and Riddiford, 1981). Advances in molecular biology and transcriptomic technologies have fueled the identification of a growing number of genes encoding OBPs in many orders of insects, including Coleoptera (e.g., 39 OBPs in *Phyllotreta striolata*, Xiao et al., 2023), Hemiptera (e.g., 49 OBPs in *Riptortus pedestris*, Li L. L. et al. (2022)), Diptera (e.g., 28 OBPs in *Liriomyza trifolii*, Zhang et al. (2022)), Lepidoptera (e.g., 31 OBPs in *Chilo sacchariphagus*, Liu et al. (2021a)), Hymenoptera (e.g., 21 OBPs in *Apis mellifera*, Forêt and Maleszka (2006)), Orthoptera (e.g., 22 OBPs in *Locusta migratoria*, Pelosi et al. (2018)). Experimental efforts have revealed that OBPs which are primarily expressed in the antennae of certain insects are capable of interacting with specific chemical ligands including host volatiles and pheromones (Zhang et al., 2020a; Rihani et al., 2021). AlepOBP6,

for instance, is predominantly expressed in the antennae of male *Athetis lepigone* individuals and can recognize both maize-derived volatile compounds and sex hormones produced by conspecific females (Li J. B. et al., 2022). In *Hippodamia variegata*, both males and females exhibit high levels of HvarOBP5 expression in their antennae, thus enabling the perception of plant and prey-derived volatiles (Tang et al., 2023). The behavioral responses of *Eupeodes corolla* to the aphid alarm pheromone (E)- $\beta$ -farnesene have been shown to be regulated by EcorOBP15 (Wang et al., 2022). Several OBPs have also been demonstrated to be expressed in other organs with or without primary chemosensory functions, including mouthpart palps (Pregitzer et al., 2018), labella (Sparks et al., 2014), legs (Hull et al., 2014), thorax (Zhang et al., 2018), and reproductive organs (Sun et al., 2012). These OBPs can facilitate a range of physiological functions including the recognition of taste compounds, the solubilization of nutrients, and the augmentation of resistance against insecticides (Pelosi et al., 2018).

*Riptortus pedestris* (Fabricius) (Hemiptera: Alydidae), known as the bean bug, is a serious agricultural pest species that is widely distributed throughout China, Japan, Korea, and other nations in East Asia (Jung and Lee, 2018; Jin et al., 2022). *R. pedestris* is a polyphagous pest species, feeding on over 30 different plants across 13 families (including Gramineae, Cruciferae, and other crop families), although they exhibit a particular preference for soybeans and other leguminous plants (Mainali et al., 2014; Ahn et al., 2020). Large numbers of these bean bugs typically infest soybean fields in the late flowering or early pod-growing stages and persistently feed on and damage these plants until harvest time (Endo et al., 2011). Soybean leaves, stems, pods, and flowers can be damaged by both *R. pedestris* adults and nymphs through their piercing and sucking behaviors, resulting in leaf rolling, stunted growth, and seed pods that are shriveled or empty, culminating in serious reductions in soybean quality and yield (Ahn et al., 2020). *R. pedestris*-associated soybean damage has recently emerged as a particularly serious problem in the Huang-Huai-Hai region of China (Li L. L. et al., 2022). Soybean plants in this region often suffer from the staygreen phenomenon that can be caused by *R. pedestris* feeding, which results in leaves that remain green, shriveled pods, and maturity stage seed abortion in soybean plants (Li et al., 2019; Dong et al., 2022). The control of *R. pedestris* has traditionally been achieved through the application of pyrethroids or other broad-spectrum insecticides (Gao et al., 2019; Guo et al., 2023). Such insecticide-based management practices, however, entail many potentially serious issues including environmental pollution, elevated levels of insecticide resistance, and inadequate efficacy owing to the highly mobile nature of these insects and their behavioral avoidance of insecticides (Bae et al., 2019; Zhu et al., 2022). There is thus a pressing need to develop new, ecologically friendly olfaction-based strategies for the control of *R. pedestris* infestations.

*R. pedestris* rely on their highly-developed antennae harboring abundant sensilla to detect both adult male-derived aggregation pheromone and host plant-derived volatiles, thus facilitating conspecific and host location efforts (Leal et al., 1995; Kim et al., 2016; Roh et al., 2021; Song et al., 2022). Li J. B. et al. (2022) previously analyzed the *R. pedestris* genome and identified 49 candidate RpedOBPs, including RpedOBP38, which exhibited high levels of expression in the antennae. The specific involvement

of RpedOBP38 in the detection of host volatiles or other chemical signals, however, has yet to be documented. Accordingly, this study was devised to clarify the olfactory functions of RpedOBP38. To that end, the sequence of the *RpedOBP38* gene was initially analyzed, after which *RpedOBP38* expression was analyzed across a variety of tissues and developmental stages via real-time quantitative PCR (qRT-PCR). The binding affinity of RpedOBP38 for 36 volatiles (including 11 green leaf volatiles, 11 soybean volatiles, 10 volatiles associated with repellent activity, and 4 aggregation pheromone compounds) was characterized through a fluorescence binding assay. Lastly, homology modeling and molecular docking approaches were used to characterize the binding sites and key amino acids related to the ligand binding activity of RpedOBP38. Together, the results of these analyses provide a robust evidence base for the further molecular characterization of the mechanisms governing olfactory recognition in *R. pedestris*, thus supporting efforts to improve the integrated management of this economically significant pest species.

## 2 Materials and methods

### 2.1 Insect rearing and tissue collection

*R. pedestris* specimens were captured in July–August 2019 from soybean fields in Shijiazhuang, Hebei province, China. Adults and nymphs were reared as in prior reports (Guo et al., 2023). Briefly, these insects were housed at 26°C ± 1°C under 60% ± 5% relative humidity (RH) with a 16 h: 8 h (L:D) photoperiod in cages, and were fed dried seeds (variety Jidou 12) and soybean seedlings that were replaced every 5–7 days. Based on the study of Li L. L. et al. (2022), 3-day-old virgin male and female adults were processed to collect antennae (40 pairs), heads without antennae (from 10 individuals), thoraxes (from 4 individuals), abdomens (from 3 individuals), wings (from 40 individuals), and legs (from 20 individuals). In addition, antennae were collected from 2nd (200 pairs), 3rd (120 pairs), 4th (60 pairs), and 5th (60 pairs) instar nymphs, after which they were snap-frozen with liquid nitrogen and stored at –80°C.

### 2.2 Total RNA extraction and preparation

TRIzol (TransGen, China) was used to extract RNA according to the manufacturer's instructions, the quality of which was analyzed via 1.0% agarose gel electrophoresis and spectrophotometry with a NanoDrop™ 2000 instrument (Thermo Fisher Scientific, United States). Next, 1 µg of the extracted RNA was processed with All-in-One First-Strand cDNA Synthesis SuperMix (TransGen), and the resultant cDNA was stored at –20°C.

### 2.3 Sequence alignment and phylogenetic analyses

The SignalP 6.0 server (<https://services.healthtech.dtu.dk/services/SignalP-6.0/>) was used for signal peptide prediction, while ClustalX 2.0 was used for multiple alignment of the RpedOBP38 protein sequence and those of other Hemiptera

OBPs, with GeneDoc (<http://nrbsc.org/gfx/genedoc>) being used for result visualization. The amino acid sequences of other hemipteran species were downloaded by accessing the NCBI website. MEGA7 was used to construct a phylogenetic tree with the neighbor-joining method and bootstrap testing (1,000 replicates). The Poisson correction method was employed when calculating evolutionary distance.

### 2.4 RpedOBP38 expression profiles

*RpedOBP38* expression was validated via qRT-PCR with an ABI QuantStudio6 Q6 Real-Time PCR System (Applied Biosystems, CA, United States) using primers designed with Premier 6 and prepared by Sangon Biotech Co., Ltd (Beijing, China) (Supplementary Table S1). Individual 20 µL reactions comprised 1 µL of cDNA, 0.6 µL each of F/R primers (10 µM), 10 µL of 2 × FastFire qPCR PreMix (TianGen Biotech, Beijing, China), and 7.8 µL of ddH<sub>2</sub>O. Reaction settings were: 94°C for 30 s; 40 cycles of 94°C for 5 s, 55°C for 15 s, and 72°C for 10 s. Relative *RpedOBP38* expression was assessed with the 2<sup>–ΔΔCt</sup> method, using *EF1* and *Actin* as reference genes (Wang et al., 2023). Three independent biological replicates were analyzed per sample.

### 2.5 Recombinant plasmid construction

The *RpedOBP38* open reading frame (ORF) lacking a signal peptide sequence was PCR amplified with TransStart® FastPfu PCR SuperMix (TransGen Biotech). Primers used to construct an RpedOBP38 expression vector were as follows: Forward: 5'-GAT GAGGCGAAACAGATG-3', Reverse: 5'-TCACTGTAGATCTTC AGTTCC-3'. Amplification settings were as follows: 95°C for 1 min; 35 cycles of 95°C for 20 s, 55°C for 20 s, and 72°C for 1 min; 72°C for 5 min. The products of PCR amplification were ligated into the pEASY-Blunt E1 vector (TransGen Biotech) and transformed into *E. coli* Trans-T1. Sangon Biotech then sequenced and confirmed the amplified gene products, and positive recombinant pEASY-Blunt E1-RpedOBP38 plasmids were obtained for further use.

### 2.6 Recombinant RpedOBP38 purification

After transforming *E. coli* BL21 (DE3) with recombinant RpedOBP38 expression vectors, positive clones were isolated and used to initiate cultures in LB broth containing 50 µg/mL ampicillin that were incubated at 37°C and 220 rpm. When the OD<sub>600</sub> reached 0.6, 1 mM of isopropyl β-D-thiogalactoside (IPTG) was added and bacteria were incubated under the same conditions for a further 6 h. Cells were then centrifuged (8,000 xg, 4°C) and resuspended in 20 mL of PBS (pH 7.0). Cells were then ultrasonically disrupted, and homogenates were centrifuged (14,000 rpm, 20 min, 4°C). The supernatants were then assessed via 12% SDS-PAGE separation. Target proteins from the supernatant fractions were applied to a Ni-chelating affinity column (GE, United States), which was subsequently equilibrated with 100 mM NaCl, 20 mM Tris-HCl, pH 7.9, and eluted using an ascending imidazole concentration

series (50, 100, 150 and 200 mM). Dialysis was used to desalt the eluent, and target protein size and purity were assessed via SDS-PAGE. Recombinant protein concentrations were measured via Bradford assay.

## 2.7 Fluorescence competitive binding assay

Recombinant RpedOBP38 binding to putative chemical ligands was characterized with a microplate reader (BioTek Synergy H1, United States). Fluorescence intensity values at the excitation wavelength of 337 nm and a maximum fluorescence emission wavelength of 450 nm were plotted against the free concentration of ligand for the measurement of dissociation constants, selecting candidate ligands from among 36 volatile compounds that included 11 green leaf volatiles (Chen et al., 2018; Guo and Wang, 2019; Cheng et al., 2020; Hong et al., 2022; Tang et al., 2023; Zhu et al., 2023), 11 soybean volatiles (Wang et al., 2019a; Zhu et al., 2022), 10 repellent activity volatiles (Zhang et al., 2013; Zhang et al., 2014), and 4 aggregation pheromone compounds (Leal et al., 1995; Yasuda et al., 2007). HPLC-grade methanol was used for the dissolution of the probe N-phenyl-1-naphthylamine (1-NPN) and all ligands. The ability of RpedOBP38 to bind 1-NPN was assessed by using 10 mM PBS (pH 7.4) to prepare a 2  $\mu$ M purified protein solution, titrating with 1 mM 1-NPN in methanol to prepare final concentrations from 2–20  $\mu$ M. RpedOBP38 binding to each ligand was evaluated in a solution consisting of 2  $\mu$ M purified protein and 1-NPN, followed by titration through the addition of ligands until no further decrease in the fluorescence intensity was observed. Ligands were independently replicated three times, and dissociation constants for each ligand were measured as follows:  $K_i = [IC_{50}]/(1 + [1-NPN]/K_{1-NPN})$ , where  $IC_{50}$  denotes the ligand concentration when the fluorescence intensity is half of the initial value [1-NPN] is the free 1-NPN concentration, and  $K_{1-NPN}$  is the dissociation constant for the RpedOBP38/1-NPN complex (Campanacci et al., 2001). Based on the study of Cui et al. (2018), the strength of binding affinity could be indicated by  $K_i$  value, including very strong ( $K_i < 6 \mu$ M), strong ( $6 \mu$ M  $\leq K_i < 22 \mu$ M), moderate ( $22 \mu$ M  $\leq K_i < 40 \mu$ M) and weak ( $K_i > 40 \mu$ M).

## 2.8 Homology modelling and molecular docking analyses

RpedOBP38 tertiary structure modeling was performed with the I-TASSER server (Zheng et al., 2021), due to the <30% homology with the protein sequences in the Swiss-model server. The RpedOBP38 amino acid sequence was utilized as an input, utilizing the 10 template proteins exhibiting the highest sequence identity for the purposes of modeling (Supplementary Table S2). C-score values were used to choose the best model from among the top 5 (Supplementary Table S3), with C-scores generally falling in the [-5, 2] range, and higher scores being indicative of greater model confidence. For the chosen ligands, the PubChem database (<https://pubchem.ncbi.nlm.nih.gov/>) was accessed to download 3D structures that were subsequently converted into the mol2 format with Open Babel GUI v.3.1.1 (O'Boyle et al., 2011). Molecular docking analyses of the interactions between RpedOBP38 and

seven ligands were performed with AutoDock Vina (v.1.1.2) (Trott and Olson, 2010) using default parameters. PyMOL v.2.0 (Schrödinger, LLC) was used for the visualization of the molecular docking results, and interaction forces were examined with PLIP (<https://plip-tool.biotec.tu-dresden.de/plipweb/plip/index>).

## 2.9 Statistical analyses

RpedOBP38 expression was analyzed across various *R. pedestris* tissues and developmental stages using one-way ANOVA with Tukey's multiple comparison test.  $p < 0.05$  was selected as the cut-off for significance, and SPSS 20.0 (IBM 2011) was used for all statistical analyses, while GraphPad Prism 8.0 was used for figure generation.

## 3 Results

### 3.1 RpedOBP38 sequence analyses

RpedOBP38 cDNA sequences were downloaded from the *R. pedestris* genome (Li J. B. et al., 2022). The RpedOBP38 ORF was found to consist of 462 bp encoding a 153-amino-acid (aa) protein, with a 19-aa N-terminal signal peptide. This protein had a predicted molecular mass of 15.08 kDa and a predicted isoelectric point of 5.20. BLASTp similarity analyses revealed some level of sequence identity with OBPs from other Hemiptera species, including YsigOBP15 from *Yemma signatus* (43.42%), PstaOBP3 from *Plautia stali* (38.78%), HhalOBP15 from *Halyomorpha halys* (37.50%), TeleOBP5 from *Tropidothorax elegans* (36.23%), and NvirOBP20 from *Nezara viridula* (35.71%). Phylogenetic tree analyses revealed the clustering of RpedOBP38 and YsigOBP15 from *Y. signatus* (Figure 1A). Sequence alignment also revealed the presence of six conserved cysteine residues within RpedOBP38 (Figure 1B), consistent with its classification within the classical OBP family.

### 3.2 Evaluation of RpedOBP38 expression patterns

RpedOBP38 expression across tissues and developmental stages was next characterized by qPCR, revealing significant differences in RpedOBP38 among tissues in both female ( $F_{5, 12} = 65.68, P < 0.001$ ) and male ( $F_{5, 12} = 129.09, P < 0.001$ ) adults, with the highest expression levels in the antennae of adult females and males, respectively (Figure 2A). Antennae RpedOBP38 expression levels rose with increasing developmental stages, with significant differences among stages ( $F_{5, 12} = 106.62, P < 0.001$ ), and expression levels being highest in adult antennae. However, there was no significant sex difference for RpedOBP38 expression levels (Figure 2B).

### 3.3 Characterization of RpedOBP38 binding to 1-NPN and candidate ligands

After expressing recombinant RpedOBP38 in *E. coli* BL21 (DE3), it was purified, yielding a final recombinant

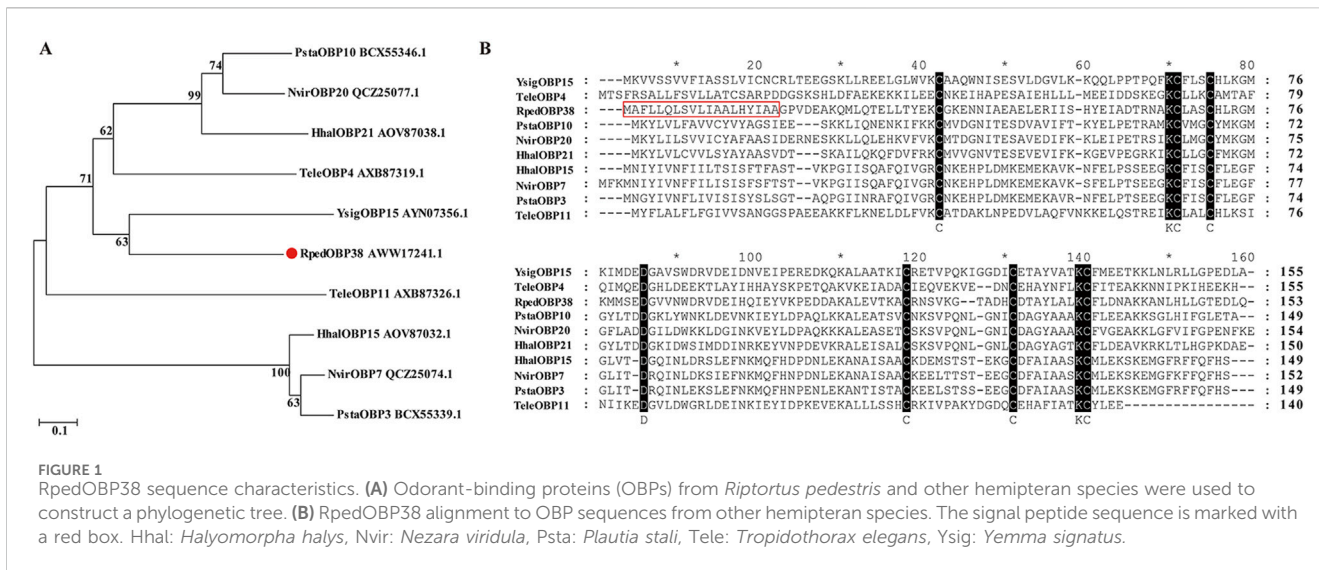


**FIGURE 1** RpedOBP38 sequence characteristics. (A) Odorant-binding proteins (OBPs) from *Riptortus pedestris* and other hemipteran species were used to construct a phylogenetic tree. (B) RpedOBP38 alignment to OBP sequences from other hemipteran species. The signal peptide sequence is marked with a red box. Hhal: *Halyomorpha halys*, Nvir: *Nezara viridula*, Psta: *Plautia stali*, Tele: *Tropidothorax elegans*, Ysig: *Yemma signatus*.

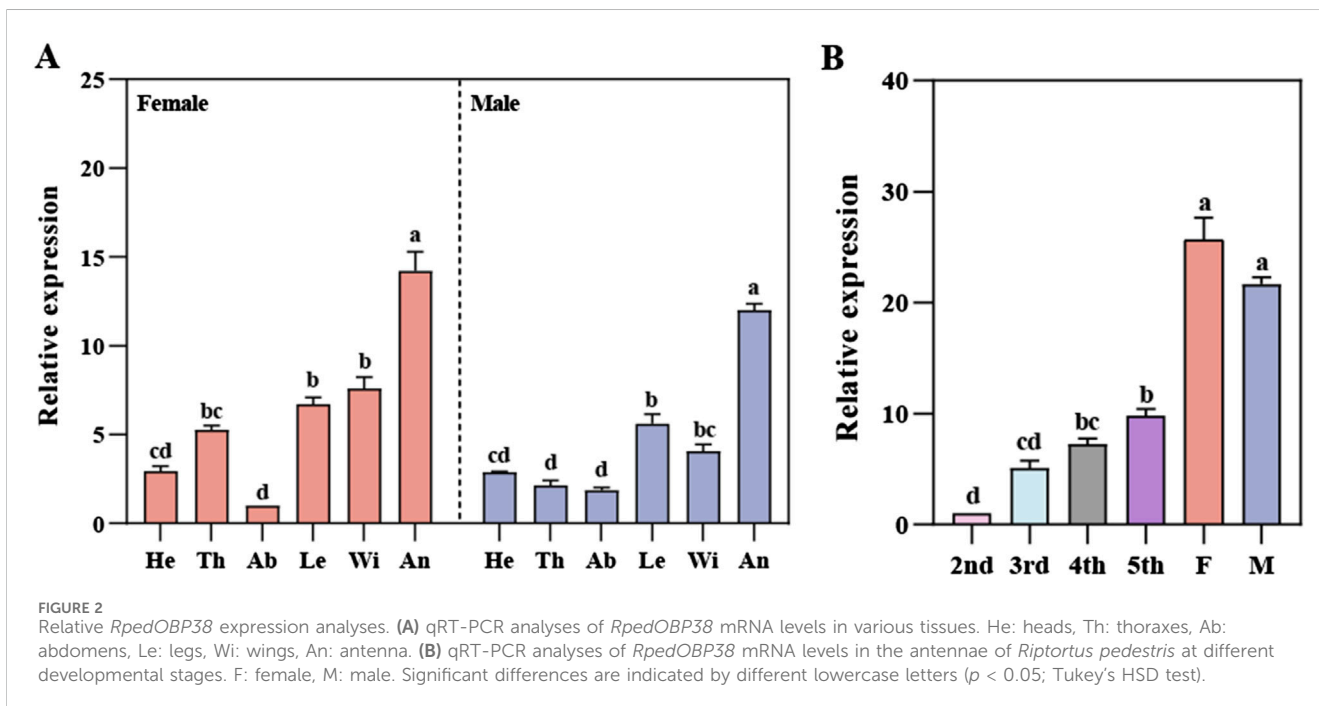


**FIGURE 2** Relative *RpedOBP38* expression analyses. (A) qRT-PCR analyses of *RpedOBP38* mRNA levels in various tissues. He: heads, Th: thoraxes, Ab: abdomens, Le: legs, Wi: wings, An: antenna. (B) qRT-PCR analyses of *RpedOBP38* mRNA levels in the antennae of *Riptortus pedestris* at different developmental stages. F: female, M: male. Significant differences are indicated by different lowercase letters ( $p < 0.05$ ; Tukey's HSD test).

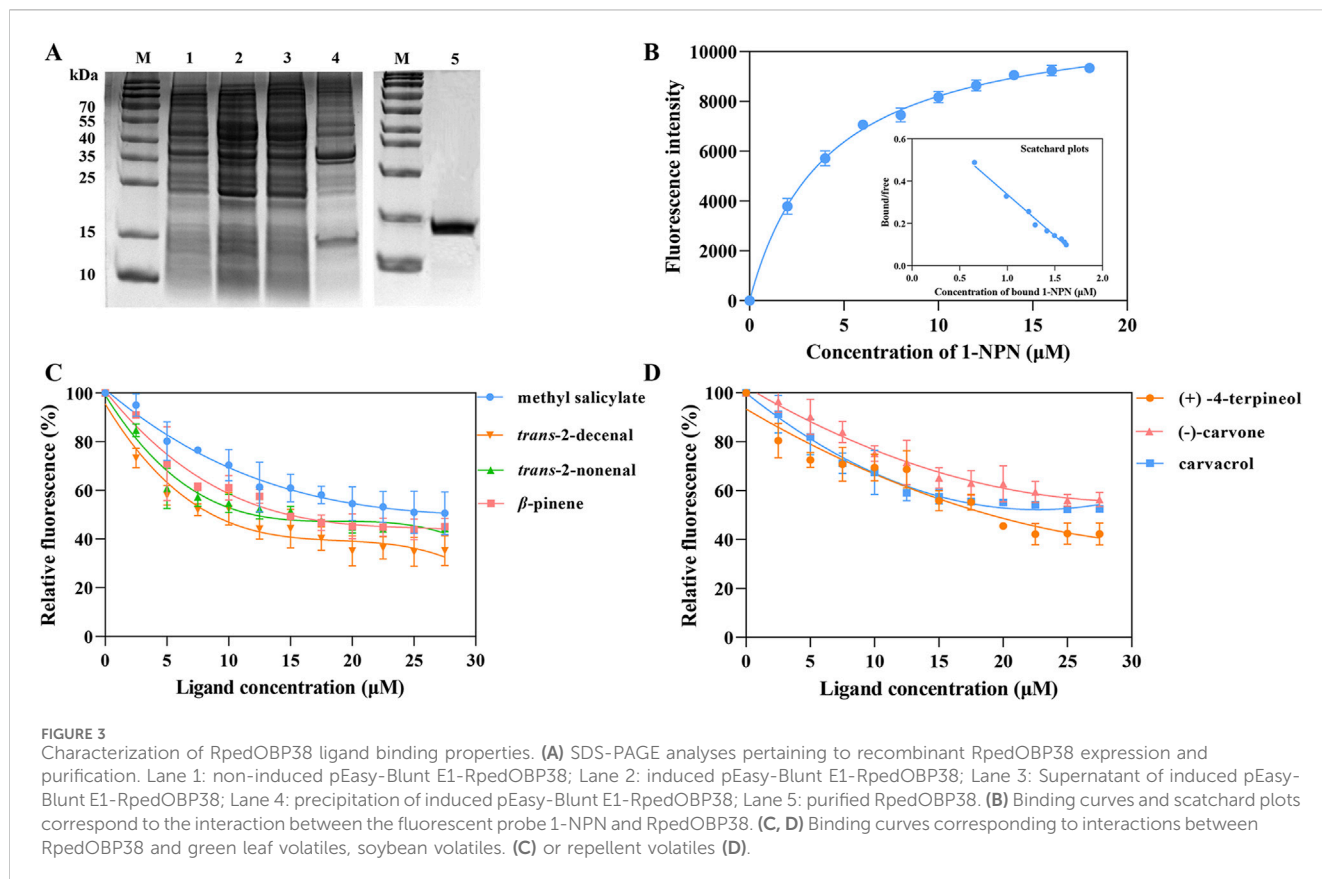
RpedOBP38 concentration of 0.603 mg/mL. SDS-PAGE analyses confirmed a similar target protein size to the predicted size (Figure 3A). The ability of RpedOBP38 to bind 1-NPN was then assessed, revealing strong binding between RpedOBP38 and 1-NPN (dissociation constant [ $K_d$ ]: 4.059  $\mu\text{mol/L}$ ). Binding curve analyses and Scatchard plots revealed the presence of a single binding site, indicating that 1-NPN was a highly suitable probe for subsequent binding analyses (Figure 3B).

In total, 36 volatile compounds including 11 green leaf volatiles, 11 soybean volatiles, 10 volatiles associated with repellent activity, and 4 aggregation pheromone compounds were chosen for the evaluation of RpedOBP38 ligand binding. The resultant analyses demonstrated the ability of RpedOBP38 to strongly bind to the soybean volatiles *trans*-2-decenal ( $K_i = 7.440 \mu\text{M}$ ), *trans*-2-nonenal

( $K_i = 10.973 \mu\text{M}$ ) and methyl salicylate ( $K_i = 21.065 \mu\text{M}$ ) (Figure 3C; Table 1). It also exhibited strong or moderate binding to three volatiles associated with repellent activity (+) -4-terpineol, ( $K_i = 14.017 \mu\text{M}$ ; carvacrol,  $K_i = 19.446 \mu\text{M}$ ; (-)-carvone,  $K_i = 27.215 \mu\text{M}$ ) (Figure 3D; Table 1). In contrast, it exhibited weak binding activity for the tested aggregation pheromone compounds ( $K_i > 40 \mu\text{M}$ ) (Table 1).

### 3.4 Homology modeling and molecular docking analyses

When the I-TASSER server was used to construct 3D models of the structure of RpedOBP38, the first model among the top five



generated models exhibited the highest C-score of  $-1.13$  (Supplementary Table S3). This predicted RpedOBP38 model contained six  $\alpha$ -helices designated  $\alpha 1$  (Pro21-Glu42),  $\alpha 2$  (Glu47-Ser55),  $\alpha 3$  (Cys67-Gly75),  $\alpha 4$  (Trp87-Glu97),  $\alpha 5$  (Pro101-Ala113), and  $\alpha 6$  (His124-Ala142) that were folded around a hydrophobic cavity. It also harbored three interlocking disulfide bridges formed by links between Cys39 in  $\alpha 1$  and Cys71 in  $\alpha 3$ , Cys67 in  $\alpha 3$  and Cys125 in  $\alpha 6$ , and Cys114 in  $\alpha 5$  and Cys134 in  $\alpha 6$ , providing further stability to the hydrophobic structure of this protein (Figure 4A).

Based on the fluorescence competitive binding assays performed above,  $\beta$ -pinene, methyl salicylate, *trans*-2-nonanal, *trans*-2-decenal (+) -4-terpineol (-)-carvone, and carvacrol were chosen as target ligands for molecular docking analyses. All seven of these ligands exhibited negative binding energy values when interacting with RpedOBP38 ranging from  $-5.71$  to  $-4.20$  (Table 2). Hydrogen bonds, hydrophobic interactions, and  $\pi$ -stacking were all found to contribute to these RpedOBP38-ligand binding interactions (Figures 4B–H). Both polar (e.g., Lys133, Glu97, His 94, Thr31) and nonpolar (e.g., Ile59, Leu136, Val85, Phe135) residues within the hydrophobic RpedOBP38 cavity were found to contribute to intermolecular binding interactions. Some of these amino acid residues were found to bind to multiple ligands, including 10 (Glu32, Ile59, Val85, Ile96, Thr111, Tyr129, Ala131, Lys133, Phe135, and Leu136) that were able to bind to three ligands, and 5 (Leu29, Thr31, Ile93, His94, and Glu97) that were able to bind to three ligands (Table 2).

## 4 Discussion

OBPs have been identified across many insect species to date and have been confirmed to be integral to the recognition of exogenous chemical signals and the regulation of physiological activities (Venthur and Zhou, 2018). OBPs have been established as promising molecular targets when screening for odorous compounds with attractant or repellent properties, informing the development of push-pull pest control strategies (Zhang et al., 2021; Song et al., 2022; Zhu et al., 2022; Zhu et al., 2023). For instance, CquiOBP1 of *Culex quinquefasciatus* was used as a target to guide the successful synthesis of a blend of trimethylamine and nonanal through the combination of conventional and reverse chemical ecology methodological approaches (Leal et al., 2008). The ability of certain OBPs to bind to aphid alarm pheromone has also enabled the design and synthesis of novel (*E*)- $\beta$ -farnesene analogs with repellent and insecticidal activity for *Acythosiphon pisum* (Sun et al., 2011). In light of the importance of OBPs and the rising demand for environmentally friendly approaches to managing pest species, OBPs have emerged as a research hotspot in the insect chemical ecology space.

Initial sequencing analyses performed in this study revealed that RpedOBP38 had 153 amino acids in length with a 19-aa N-terminal signal peptide and six conserved cysteine residues, consistent with its classification as a member of the classic OBP family (Pelosi et al., 2006; Brito et al., 2016). Phylogenetic analyses can be used to infer evolutionary relationships for particular genes across species,

TABLE 1 Binding affinities of all tested ligands to RpedOBP38.

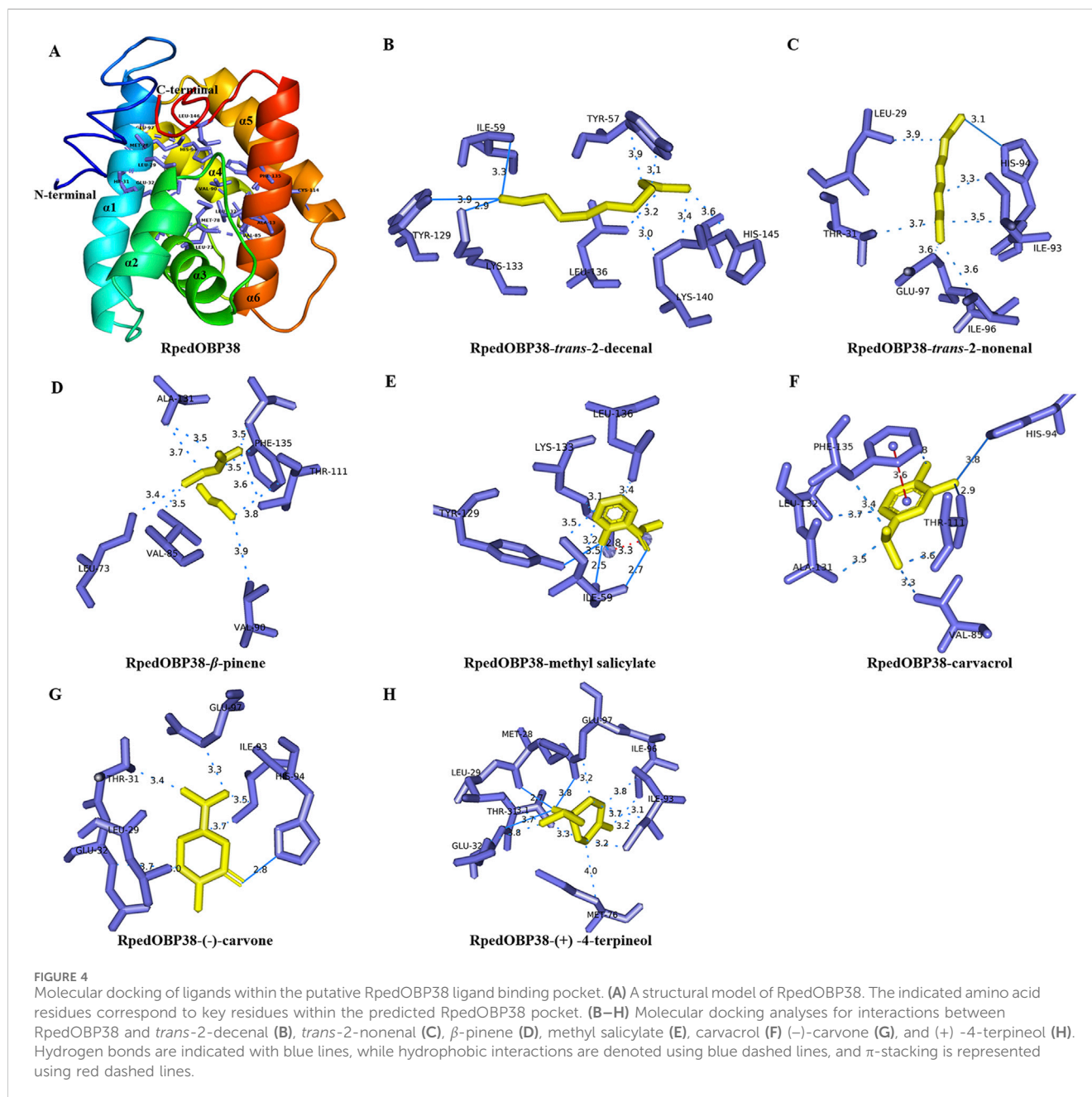
Ligands	CAS number	IC50 ( $\mu\text{mol/L}$ )	Ki ( $\mu\text{mol/L}$ )
<b>Green leaf volatiles</b>			
<i>trans</i> -2-hexenal	6,728-26-3	>40	>40
octanal	124-13-0	>40	>40
nonanal	124-19-6	>40	>40
$\beta$ -myrcene	123-35-3	>40	>40
<i>trans</i> -caryophyllene	87-44-5	>40	>40
$\alpha$ -pinene	13,877-91-3	>40	>40
geraniol	106-24-1	>40	>40
camphene	565-00-4	>40	>40
$\beta$ -pinene	127-91-3	16.393 $\pm$ 0.261	12.315 $\pm$ 0.196
(+)- $\alpha$ -pinene	7,785-70-8	>40	>40
(-)- $\alpha$ -pinene	7,785-26-4	>40	>40
<b>Soybean volatiles</b>			
hexanal	66-25-1	>40	>40
1-hexanol	111-27-3	>40	>40
1-octen-3-ol	3,391-86-4	>40	>40
3-octanone	106-68-3	>40	>40
<i>cis</i> -3-hexen-1-ol	928-96-1	>40	>40
<i>cis</i> -3-hexenyl acetate	3,681-71-8	>40	>40
methyl salicylate	119-36-8	28.039 $\pm$ 5.938	21.065 $\pm$ 4.461
<i>trans</i> -2-hexenyl acetate	2,497-18-9	>40	>40
<i>trans</i> -2-octenal	2,548-87-0	>40	>40
<i>trans</i> -2-nonenal	18,829-56-6	14.606 $\pm$ 0.821	10.973 $\pm$ 0.617
<i>trans</i> -2-decenal	3,913-81-3	9.904 $\pm$ 0.970	7.440 $\pm$ 0.729
<b>Volatiles with repellent activity</b>			
eugenol	97-53-0	>40	>40
isoeugenol	97-54-1	>40	>40
(-) -4-terpineol	20,126-76-5	>40	>40
(+) -4-terpineol	2,438-10-0	18.658 $\pm$ 0.428	14.017 $\pm$ 0.321
$\gamma$ -terpinene	99-85-4	>40	>40
cineole	470-82-6	>40	>40
$\alpha$ -terpinene	99-86-5	>40	>40
(-)-carvone	6,485-40-1	36.226 $\pm$ 5.169	27.215 $\pm$ 3.883
(+)-carvone	2,244-16-8	>40	>40
carvacrol	499-75-2	25.898 $\pm$ 0.443	19.456 $\pm$ 0.333
<b>Pheromone compounds</b>			
<i>trans</i> -2-hexenyl hexanoate	53,398-86-0	>40	>40
(E)-2-hexenyl (Z)-3-hexenoate (E2-6:Z3Hex)	53,398-87-1	>40	>40

(Continued on following page)

TABLE 1 (Continued) Binding affinities of all tested ligands to RpedOBP38.

Ligands	CAS number	IC50 ( $\mu\text{mol/L}$ )	Ki ( $\mu\text{mol/L}$ )
(E)-2-hexenyl (Z)-2-hexenoate (E2-6:E2Hex)	54,845-28-2	>40	>40
myristyl isobutyrate	167,871-30-9	>40	>40

'Ki > 40  $\mu\text{M}$ ' means that the binding ability of RpedOBP38 recombinant protein to this ligand was considered weak.



thereby informing functional analyses such that they have been widely used for characterizing insect OBPs (Chen et al., 2018; Zhang et al., 2022; Tang et al., 2023; Zhu et al., 2023). In this study, RpedOBP38 and YsigOBP15 from *Y. signatus* clustered together, suggesting their evolution from a shared ancestor and their potential for similar physiological functions. Analyzing the patterns of insect

OBP expression across developmental stages and tissues is vital for the clarification of the physiological functions of these factors (Ju et al., 2014; Wang et al., 2019b; Li et al., 2020). In general, OBPs are likely to play a role in the recognition of chemical signals if they are expressed at high levels in antennae and other olfactory organs (Chen et al., 2018; Li et al., 2020; Hong et al., 2022; Zhang et al., 2022;



TABLE 2 Prediction of key amino acid residues involved in the docking of RpedOBP38 to different ligands.

Ligands	Binding energy (kcal/mol)	Closer contact interacting residues
$\beta$ -pinene	-5.07	LEU73, VAL85, VAL90, THR111, ALA131, PHE135
methyl salicylate	-5.42	<b>ILE59</b> , <b>TYR129</b> , <b>LYS133</b> , <i>LYS133</i> , LEU136
<i>trans</i> -2-nonenal	-4.20	LEU29, THR31, ILE93, <b>HIS94</b> , ILE96, GLU97
<i>trans</i> -2-decenal	-5.17	TRY57, <b>ILE59</b> , <b>TYR129</b> , <b>LYS133</b> , LEU136, LYS140, HIS145
(+)-4-terpineol	-5.30	<b>MET28</b> , LEU29, THR31, <b>GLU32</b> , MET76, ILE93, ILE96, <b>GLU97</b>
(-)-carvone	-5.71	LEU29, THR31, GLU32, ILE93, <b>HIS94</b> , GLU97
carvacrol	-5.52	VAL85, <b>HIS94</b> , <b>THR111</b> , ALA131, LEU132, <i>PHE135</i>

Amino acids in bold font represent hydrogen bond, amino acids in italic represent  $\pi$ -stacking, and other amino acids represent hydrophobic interaction.

Tang et al., 2023). Higher levels of *RpedOBP38* expression were noted in the antennae relative to other tissues in this study, with no significant difference between females and males. This result was in line with a prior report by Li L. L. et al (2022), indicating that *RpedOBP38* may play an important role in the recognition of host volatiles and/or aggregation pheromones by *R. pedestris*. Other groups have also reported similar outcomes. For instance, Huang et al. (2018) reported the specific expression of AipsOBP2 in *Agrotis ipsilon* antennae and found that it was capable of binding both host volatiles and sex pheromones. Cheng et al. (2020) additionally noted the strong binding of SmosOBP12, which was expressed at high levels in the antennae of female *Sitodiplosis mosellana*, to host volatiles derived from wheat including hexyl acetate and 3-hexanol. *R. pedestris* reportedly harbor many different olfactory sensors on their antennae (Kim et al., 2016), and are attracted to soybean-derived volatile compounds and aggregation pheromones released by conspecific males (Leal et al., 1995; Song et al., 2022). High levels of *RpedOBP38* expression were also noted in the adult stage, suggesting its potential involvement as a mediator of soybean volatile and aggregation pheromone recognition in *R. pedestris*.

Given the role that OBPs play as carriers in the context of chemical communication in insects, there is a need to clarify the affinity of these compounds for exogenous organic factors including pheromones and host-derived odors, thereby potentially offering insight into the structural features of cognate ligands to guide reverse chemical ecology studies (D'Onofrio et al., 2020). Fluorescence competitive binding have been established as a reliable means of assessing *in vitro* binding between OBPs and their ligands (He et al., 2019; D'Onofrio et al., 2020). This approach has been successfully implemented across various species of insects including *Diaphorina citri* (Liu et al., 2021b), *Liomyza trifolii* (Zhang et al., 2022), *R. pedestris* (Zhu et al., 2022), *Bradysia odoriphaga* (Zhu et al., 2023), and *Hippodamia variegata* (Tang et al., 2023). In this study, the ability of *RpedOBP38* to bind to 11 green leaf volatiles, 11 soybean volatiles, 10 volatiles with repellent activity, and 4 aggregation pheromone compounds was assessed. In total, it was found to bind to three soybean volatiles (*trans*-2-decenal, *trans*-2-nonenal, methyl salicylate) and one green leaf volatile ( $\beta$ -pinene). Host plant volatiles have been shown to promote feeding, avoidance, oviposition, and a range of other behavioral responses (Anderson et al., 1993; Leal et al., 1994; Zhu et al., 2022). *RpedOBP38* may thus play a role in the detection of soybean volatiles, although behavioral and RNA interference assays will be necessary to confirm this

hypothesis. Zhu et al. (2022) previously demonstrated the ability of *RpedOBP4* to bind other soybean volatiles including 1-hexanol and *trans*-2-hexenyl acetate, supporting the potential involvement of multiple OBPs in the process of host plant recognition in line with what has been reported by Li et al. (2017). *RpedOBP38* was also able to bind less strongly to plant essential oil-derived volatiles with repellent activity ((+) -4-terpineol (-)-carvone, carvacrol) that exhibit high levels of repellency for various insect species (Quintana et al., 2009; Zhang et al., 2014). However, the binding affinity of *RpedOBP38* for tested aggregation pheromones was low ( $K_i > 40 \mu\text{M}$ ), suggesting that binding to these compounds may be primarily mediated by other chemosensory proteins including *RpedCSP12* (Yin et al., 2023). Notably, *RpedOBP38* exhibited distinct binding affinity levels for certain isomers as in the case of (+) -4-terpineol ( $K_i = 14.02 \mu\text{M}$ ) and (-) -4-terpineol ( $K_i > 40 \mu\text{M}$ ), or (-)-carvone ( $K_i = 27.22 \mu\text{M}$ ) and (+)-carvone ( $K_i > 40 \mu\text{M}$ ). Factors including carbon chain length, conformational changes, and structural features can thus likely shape *RpedOBP38* binding affinity (Chen et al., 2018; Hong et al., 2022).

The physiological functions of a given protein are determined by its 3D structure, and insect OBPs generally harbor a hydrophobic cavity formed from multiple  $\alpha$ -helices, with some of the amino acids therein facilitating interactions between these OBPs and their ligands (He et al., 2019; Zhang et al., 2020b; Yang et al., 2021; Zhu et al., 2023). Molecular modeling analyses performed herein revealed the presence of a hydrophobic binding pocket within *RpedOBP38* that was stabilized by six  $\alpha$ -helices and three interlocking disulfide bridges. This is consistent with similar reports for *DcitOBP7* in *Diaphorina citri* (Liu et al., 2021a), and *PyasOBP2* in *Pachyrhinus yasumatsui* (Hong et al., 2022), suggesting that they may engage in similar ligand-binding mechanisms. Molecular docking analyses revealed negative binding energy values for interactions between *RpedOBP38* and seven analyzed ligands, implying strong protein-ligand interactions, consistent with the fluorescence competitive binding assay results. OBP-ligand binding is generally mediated by types of intermolecular forces including hydrogen bonds, van der Waals interactions, and hydrophobic interactions (Zhuang et al., 2014; Li et al., 2021; Hong et al., 2022). In this study, hydrogen bonds, hydrophobic interactions, and  $\pi$ -stacking were all found to shape *RpedOBP38*-ligand interactions, with molecular docking analyses also revealing the distribution of several polar (e.g., Lys133, Glu97, His 94, Thr31) and nonpolar (e.g., Ile59, Leu136, Val85, Phe135) residues within

the RpedOBP38 hydrophobic pocket jointly contributing to such intermolecular binding. This aligns well with other reports for insect OBPs, including the Val114, Thr9, and Val111 residues in *Grapholita molesta* OBP2 (Li et al., 2016), Tyr77, Ile41, Ala116, and Lys38 in *Apibid Sitobion* OBP9 (Ullah et al., 2020), Leu33, Phe8, Met76, Ile30, Tyr47, Asp29, and Lys120 in *R. pedestris* OBP4 (Zhu et al., 2022), and Lys43, His64, and Leu42 in *H. variegata* OBP5 (Tang et al., 2023). Some of these amino acids were found to be capable of binding to more than one ligand, including Leu29, Thr31, His94, Glu97, Ile59, and Lys133, in line with what has previously been described in both *Athetis lepigone* (Li L. L. et al., 2022) and *R. pedestris* (Zhu et al., 2022). These residues may thus be particularly important mediators of RpedOBP38-ligand binding, highlighting an opportunity for site-directed mutagenesis to validate this hypothesis in the future (Zhu et al., 2020).

In summary, these experiments revealed that RpedOBP38, which was highly expressed in the antennae of adult *R. pedestris*, is a classical OBP family member that clusters most closely with YsigOBP15 from *Y. signatus*. Fluorescence competitive binding analyses demonstrated the ability of RpedOBP38 to bind strongly to two soybean volatiles (*trans*-2-decenal,  $K_i = 7.440 \mu\text{M}$ ; *trans*-2-nonenal,  $K_i = 10.973 \mu\text{M}$ ; methyl salicylate,  $K_i = 21.065 \mu\text{M}$ ) and to bind strongly or moderately to volatiles associated with repellent activity ((+) -4-terpineol,  $K_i = 14.017 \mu\text{M}$ ; carvacrol,  $K_i = 19.456 \mu\text{M}$ ; (-)-carvone,  $K_i = 27.215 \mu\text{M}$ ). Through 3D modeling and molecular docking analyses, RpedOBP38 was found to harbor six  $\alpha$ -helices that form a stable hydrophobic binding pocket, with the Leu29, Thr31, His94, Glu97, Ile59, and Lys133 amino acid residues all playing key roles in the ability of this OBP to bind its ligands. Together, these results offer further insight into the mechanisms that govern olfactory recognition in *R. pedestris*. In order to more deeply elucidate the function of RpedOBP38, future studies are planned to analyse the exact role of RpedOBP38 in the recognition of more green leaf volatiles and soybean volatiles using a combination of behavioural experiments, electrophysiological experiments, and RNA inference (Zhu et al., 2022). Furthermore, we attempt to use RpedOBP38 as a control target, devise ecologically friendly behavioural inhibitors to disrupt the feeding behavior of *R. pedestris* and thus improve the management of *R. pedestris* (Zhu et al., 2022).

## Data availability statement

The datasets presented in this study can be found in online repositories. The names of the repository/repositories and accession number(s) can be found in the article/Supplementary Material.

## Ethics statement

The manuscript presents research on animals that do not require ethical approval for their study.

## Author contributions

JG: Data curation, Formal Analysis, Funding acquisition, Visualization, Writing—original draft. PL: Methodology, Software, Validation, Visualization, Writing—original draft. XZ: Data curation, Formal Analysis, Software, Writing—original draft. JA: Data curation, Formal Analysis, Resources, Validation, Writing—review and editing. YL: Data curation, Validation, Writing—review and editing. TZ: Conceptualization, Investigation, Project administration, Writing—review and editing. ZG: Conceptualization, Funding acquisition, Investigation, Supervision, Writing—review and editing.

## Funding

The author(s) declare that financial support was received for the research, authorship, and/or publication of this article. This work was supported by National Natural Science Foundation of China (32302358), HAAFS Agriculture Science and Technology Innovation Project (2022KJCXZX-ZBS-4), Natural Science Foundation of Hebei Province (C2022301052), and Key research and Development Program of Hebei Province (22326513D).

## Acknowledgments

We would like to thank all the reviewers who participated in the review during the preparation of this manuscript. We are also grateful to Hui-Fang Zhou from the Plant Protection Institute, Hebei Academy of Agricultural and Forestry Sciences, for her contribution in insect collection.

## Conflict of interest

The authors declare that the research was conducted in the absence of any commercial or financial relationships that could be construed as a potential conflict of interest.

## Publisher's note

All claims expressed in this article are solely those of the authors and do not necessarily represent those of their affiliated organizations, or those of the publisher, the editors and the reviewers. Any product that may be evaluated in this article, or claim that may be made by its manufacturer, is not guaranteed or endorsed by the publisher.

## Supplementary material

The Supplementary Material for this article can be found online at: <https://www.frontiersin.org/articles/10.3389/fphys.2024.1475489/full#supplementary-material>

## References

- Ahmed, T., Zhang, T., Wang, Z., He, K., and Bai, S. (2017). Molecular cloning, expression profile, odorant affinity, and stability of two odorant-binding proteins in *Macrocentrus cingulum* Brischke (Hymenoptera: braconidae). *Arch. Insect Biochem.* 94 (2), e21374. doi:10.1002/arch.21374
- Ahn, J. J., Choi, K. S., and Koh, S. (2020). Population parameters and growth of *Riptortus pedestris* (Fabricius) (Hemiptera: Alydidae) under elevated CO<sub>2</sub> concentrations. *Entomol. Res.* 51 (1), 12–23. doi:10.1111/1748-5967.12479
- Anderson, P., Hilker, M., Hansson, B. S., Bomboch, S., Klein, B., and Schildknecht, H. (1993). Oviposition deterring components in larval frass of *Spodoptera littoralis* (Boisd.) (Lepidoptera: noctuidae): a behavioural and electrophysiological evaluation. *J. Insect Physiol.* 39 (2), 129–137. doi:10.1016/0022-1910(93)90104-Y
- Bae, S., Yi, H., Yoon, Y., Jang, Y., Kim, Y., and Maharjan, R. (2019). Attraction of stink bugs to rocket traps with different combinations of wing and landing board color. *J. Asia-Pac. Entomol.* 22 (1), 243–249. doi:10.1016/j.aspen.2019.01.007
- Brito, N. F., Moreira, M., and Melo, A. C. A. (2016). A look inside odorant-binding proteins in insect chemoreception. *J. Insect Physiol.* 95 (6), 51–65. doi:10.1016/j.jinphys.2016.09.008
- Campanacci, V., Krieger, J., Bette, S., Sturgis, J. N., Lartigue, A., Cambillau, C., et al. (2001). Revisiting the specificity of *Mamestra brassicae* and *Antheraea polyphemus* pheromone-binding proteins with a fluorescence binding assay. *J. Biol. Chem.* 276 (23), 20078–20084. doi:10.1074/jbc.M100713200
- Chen, X. L., Li, G. W., Xu, X. L., and Wu, J. X. (2018). Molecular and functional characterization of odorant binding protein 7 from the oriental fruit moth *Grapholita molesta* (Busck) (Lepidoptera: tortricidae). *Front. Physiol.* 9, 1762. doi:10.3389/fphys.2018.01762
- Cheng, W. N., Zhang, Y. D., Yu, J. L., Liu, W., and Zhu-Salzman, K. (2020). Functional analysis of odorant-binding proteins 12 and 17 from wheat blossom midge *Sitodiplosis mosellana* Géhin (Diptera: cecidomyiidae). *Insects* 11 (12), 891–906. doi:10.3390/insects11120891
- Cui, X. N., Liu, D. G., Sun, K. K., He, Y., and Shi, X. Q. (2018). Expression profiles and functional characterization of two odorant-binding proteins from the apple buprestid beetle *Agrilus mali* (Coleoptera: buprestidae). *J. Econ. Entomol.* 11 (3), 1420–1432. doi:10.1093/jee/toy066
- Dong, Y. M., Huang, X. G., Yang, Y. X., Li, J. F., Zhang, M. Q., Shen, H., et al. (2022). Characterization of salivary secreted proteins that induce cell death from *Riptortus pedestris* (Fabricius) and their roles in insect-plant interactions. *Front. Plant Sci.* 13, 912603. doi:10.3389/fpls.2022.912603
- D'Onofrio, C., Zaremska, V., Zhu, J., Knoll, W., and Pelosi, P. (2020). Ligand-binding assays with OBPs and CSPs. *Method. Enzymol.* 642, 229–258. doi:10.1016/bs.mie.2020.05.006
- Endo, N., Wada, T., and Sasaki, R. (2011). Seasonal synchrony between pheromone trap catches of the bean bug, *Riptortus pedestris* (Heteroptera: Alydidae) and the timing of invasion of soybean fields. *Appl. Entomol. Zool.* 46 (4), 477–482. doi:10.1007/s13355-011-0065-7
- Forêt, S., and Maleszka, R. (2006). Function and evolution of a gene family encoding odorant binding-like proteins in a social insect, the honey bee (*Apis mellifera*). *Genome Res.* 16 (11), 1404–1413. doi:10.1101/gr.5075706
- Gao, Y., Chen, J. H., and Shi, S. S. (2019). Research progress on soybean stink bug (*Riptortus pedestris*). *Chin. J. Oil Crop Sci.* 41 (5), 804–815. doi:10.19802/j.issn.1007-9084.2019033
- Guo, H., and Wang, C. Z. (2019). The ethological significance and olfactory detection of herbivore-induced plant volatiles in interactions of plants, herbivorous insects, and parasitoids. *Arthropod-Plant Inte* 13 (2), 161–179. doi:10.1007/s11829-019-09672-5
- Guo, J. L., An, J. J., Chang, H., Li, Y. F., Dang, Z. H., Wu, C., et al. (2023). The lethal and sublethal effects of lambda-cyhalothrin and emamectin benzoate on the soybean pest *Riptortus pedestris* (Fabricius). *Toxics* 11 (2), 971–989. doi:10.3390/toxics11120971
- He, P., Chen, G. L., Li, S., Wang, J., Ma, Y. F., Pan, Y. F., et al. (2019). Evolution and functional analysis of odorant binding proteins in three rice planthoppers: *Nilaparvata lugens*, *Sogatella furcifera*, and *Laodelphax striatellus*. *Pest Manag. Sci.* 75 (6), 1606–1620. doi:10.1002/ps.5277
- Hong, B., Chang, Q., Zhai, Y. Y., Ren, B. W., and Zhang, F. (2022). Functional characterization of odorant binding protein PysOBP2 from the jujube bud weevil, *Pachyrhinus yasmatsui* (Coleoptera: Curculionidae). *Front. Physiol.* 13, 900752. doi:10.3389/fphys.2022.900752
- Huang, G. Z., Liu, J. T., Zhou, J. J., Wang, Q., Dong, J. Z., Zhang, Y. J., et al. (2018). Expressional and functional comparisons of two general odorant binding proteins in *Agrotis ipsilon*. *Insect biochem. molec.* 98, 34–47. doi:10.1016/j.ibmb.2018.05.003
- Hull, J. J., Perera, O. P., and Snodgrass, G. L. (2014). Cloning and expression profiling of odorant-binding proteins in the tarnished plant bug, *Lygus lineolaris*. *Insect Mol. Biol.* 23 (1), 78–97. doi:10.1111/imb.12064
- Jin, Y., Zhang, W. D., Dong, Y. M., and Xia, A. (2022). Feeding behavior of *Riptortus Pedestris* (Fabricius) on soybean: electrical penetration graph analysis and histological investigations. *Insects* 13 (6), 511–523. doi:10.3390/insects13060511
- Ju, Q., Li, X., Jiang, X. J., Qu, M. J., Guo, X. Q., Han, Z. J., et al. (2014). Transcriptome and tissue-specific expression analysis of obp and csp genes in the Dark Black Chafer. *Arch. Insect Biochem.* 87 (4), 177–200. doi:10.1002/arch.21188
- Jung, M., and Lee, D. H. (2018). Characterization of overwintering behaviors and sites of bean bug, *Riptortus pedestris* (Hemiptera: Alydidae), under laboratory and field conditions. *Environ. Entomol.* 47 (5), 1280–1286. doi:10.1093/ee/nvy123
- Kim, J., Park, K. C., Roh, H. S., Kim, J., Oh, H. W., Kim, J. A., et al. (2016). Morphology and distribution of antennal sensilla of the bean bug *Riptortus pedestris* (Hemiptera: Alydidae): antennal sensilla of *R. pedestris*. *Microsc. Res. Tech.* 79 (6), 501–511. doi:10.1002/jemt.22658
- Leal, W. S. (2013). Odorant Reception in insects: roles of receptors, binding proteins, and degrading enzymes. *Annu. Rev. Entomol.* 58, 373–391. doi:10.1146/annurev-ento-120811-153635
- Leal, W. S., Barbosa, R. M. R., Xu, W., Ishida, Y., Syed, Z., Latte, N., et al. (2008). Reverse and conventional chemical ecology approaches for the development of oviposition attractants for *Culex mosquitoes*. *PLoS ONE* 3 (8), e3045. doi:10.1371/journal.pone.0003045
- Leal, W. S., Higuchi, H., Mizutani, N., Nakamori, H., Kadosawa, T., and Ono, M. (1995). Multifunctional communication in *Riptortus clavatus* (Heteroptera: Alydidae): conspecific nymphs and egg parasitoid *Ooencyrtus nezarae* use the same adult attractant pheromone as chemical cue. *J. Chem. Ecol.* 21 (7), 973–985. doi:10.1007/BF02033802
- Leal, W. S., Nikonova, L., and Peng, G. (1999). Disulfide structure of the pheromone binding protein from the silkworm moth, *Bombyx mori*. *FEBS Lett.* 464 (1–2), 85–90. doi:10.1016/S0014-5793(99)01683-X
- Leal, W. S., Ono, M., Hasegawa, M., and Sawada, M. (1994). Kairomone from dandelion, *Taraxacum officinale*, attractant for scarab beetle *Anomala octiescostata*. *J. Chem. Ecol.* 20 (7), 1697–1704. doi:10.1007/BF02059891
- Li, D. X., Li, C. B., and Liu, D. G. (2021). Analyses of structural dynamics revealed flexible binding mechanism for the *Agrilus mali* odorant binding protein 8 towards plant volatiles. *Pest Manag. Sci.* 77 (4), 1642–1653. doi:10.1002/ps.6184
- Li, G. W., Chen, X. L., Li, B. L., Zhang, G. H., Li, Y. P., and Wu, J. X. (2016). Binding properties of general odorant binding proteins from the oriental fruit moth, *Grapholita molesta* (Busck) (Lepidoptera: tortricidae). *PLoS ONE* 11 (5), e0155096. doi:10.1371/journal.pone.0155096
- Li, G. W., Du, J., Li, Y. P., and Wu, J. X. (2015). Identification of putative olfactory genes from the oriental fruit moth *Grapholita molesta* via an antennal transcriptome analysis. *PLoS ONE* 10 (11), e0142193. doi:10.1371/journal.pone.0142193
- Li, J. B., Yin, M. Z., Yao, W. C., Ma, S., Dewar, Y., Liu, X. Z., et al. (2022a). Genome-wide analysis of odorant-binding proteins and chemosensory proteins in the bean bug *Riptortus pedestris*. *Front. Physiol.* 13, 949607. doi:10.3389/fphys.2022.949607
- Li, K., Zhang, X. X., Guo, J. Q., Penn, H., Wu, T. T., Li, L., et al. (2019). Feeding of *Riptortus pedestris* on soybean plants, the primary cause of soybean staygreen syndrome in the Huang-Huai-Hai river basin. *Crop J.* 7 (3), 360–367. doi:10.1016/j.cj.2018.07.008
- Li, L. L., Huang, J. R., Xu, J. W., Yao, W. C., Yang, H. H., Shao, L., et al. (2022b). Ligand-binding properties of odorant-binding protein 6 in *Aethis lepigone* to sex pheromones and maize volatiles. *Pest Manag. Sci.* 78 (1), 52–62. doi:10.1002/ps.6606
- Li, M. Y., Jiang, X. Y., Qi, Y. Z., Huang, Y. J., Li, S. G., and Liu, S. G. (2020). Identification and expression profiles of 14 odorant-binding protein genes from *Pieris rapae* (Lepidoptera: pieridae). *J. Insect Sci.* 20 (5), 2–10. doi:10.1093/jisesa/ieaa087
- Li, Z. Q., Zhang, S., Cai, X. M., Luo, J. Y., Dong, S. L., Cui, J. J., et al. (2017). Three odorant binding proteins may regulate the behavioural response of *Chrysopa pallens* to plant volatiles and the aphid alarm pheromone (E)- $\beta$ -farnesene. *Insect Mol. Biol.* 26 (3), 255–265. doi:10.1111/imb.12295
- Liu, J. B., Liu, J., Yi, J. Q., Mao, Y. K., Li, J. H., Sun, D. L., et al. (2021). Transcriptome characterization and expression analysis of chemosensory genes in *Chilo sacchariphagus* (Lepidoptera Crambidae), a key pest of sugarcane. *Front. Physiol.* 12, 636353. doi:10.3389/fphys.2021.636353
- Liu, Q., Yin, M. Z., Ma, S., Gu, N., Qian, L. F., Zhang, Y. N., et al. (2023). Ligand-binding properties of chemosensory protein 1 in *Callosobruchus chinensis* to mung bean volatiles. *Pestic. Biochem. Phys.* 192, 105394. doi:10.1016/j.pestbp.2023.105394
- Liu, X. Q., Jiang, H. B., Fan, J. Y., Liu, T. X., Meng, L. W., Liu, Y., et al. (2021). An odorant-binding protein of Asian citrus psyllid, *Diaphorina citri*, participates in the response of host plant volatiles. *Pest Manag. Sci.* 77 (7), 3068–3079. doi:10.1002/ps.6352
- Mainali, B. P., Kim, H. J., Yoon, Y. N., Oh, I. S., and Bae, S. D. (2014). Evaluation of different leguminous seeds as food sources for the bean bug *Riptortus pedestris*. *J. Asia-Pacific Entomol.* 17 (2), 115–117. doi:10.1016/j.aspen.2013.11.007
- Manoharan, M., Chong, M. N. F., Vaitinadapoulé, A. G., Etienne, F., Sowdhamini, R., and Bernard, O. (2013). Comparative genomics of odorant binding proteins in *Anopheles gambiae*, *Aedes aegypti*, and *Culex quinquefasciatus*. *Genome Biol. Evol.* 5 (1), 163–180. doi:10.1093/gbe/evs131

- Martin, J. P., Beyerlein, A., Dacks, A. M., Reisenman, C. E., Riffell, J. A., Lei, H., et al. (2011). The neurobiology of insect olfaction: sensory processing in a comparative context. *Prog. Neurobiol.* 95 (3), 427–447. doi:10.1016/j.pneurobio.2011.09.007
- O'Boyle, N. M., Bank, M., James, C. A., Morley, C., Vandermeersch, T., and Hutchison, G. R. (2011). Open babel: an open chemical toolbox. *J. cheminformatics* 3 (1), 33. doi:10.1186/1758-2946-3-33
- Paula, D. P., Togawa, R., Costa, M., Grynberg, P., Martins, N. F., and Andow, D. (2018). Systemic and sex-biased regulation of OBP expression under semiochemical stimuli. *Sci. Rep.* 8 (1), 6035. doi:10.1038/s41598-018-24297-z
- Pelosi, P., Iovinella, I., Zhu, J., Wang, G., and Dani, F. (2018). Beyond chemoreception: diverse tasks of soluble olfactory proteins in insects. *Biol. Rev.* 93 (1), 184–200. doi:10.1111/brv.12339
- Pelosi, P., Mastrogiacommo, R., Iovinella, I., Tuccori, E., and Persaud, K. C. (2014). Structure and biotechnological applications of odorant-binding proteins. *Appl. Microbiol. Biot.* 98 (1), 61–70. doi:10.1007/s00253-013-5383-y
- Pelosi, P., Zhou, J., Ban, L., and Calvello, M. (2006). Soluble proteins in insect chemical communication. *Cell. Mol. Life Sci.* 63 (14), 1658–1676. doi:10.1007/s00018-005-5607-0
- Pregitzer, P., Zielonka, M., Eichhorn, A. S., Jiang, X., Krieger, J., and Breer, H. (2018). Expression of odorant-binding proteins in mouthpart palps of the desert locust *Schistocerca gregaria*. *Insect Mol. Biol.* 28 (2), 264–276. doi:10.1111/imb.12548
- Quintana, L. S. N., Olivero-Verbel, J., and Stashenko, E. (2009). Repellent activity of essential oils: a review. *Bioresour. Technol.* 101 (1), 372–378. doi:10.1016/j.biortech.2009.07.048
- Rihani, K., Ferveur, J. F., and Briand, L. (2021). The 40-year mystery of insect odorant-binding proteins. *Biomolecules* 11 (4), 509–536. doi:10.3390/biom11040509
- Roh, G. H., Cha, D. H., and Park, C. G. (2021). Olfactory attraction to aggregation pheromone is mediated by disti-flagellum of antennal segments in *Riptortus pedestris*. *J. Asia-Pacific Entomol.* 24 (1), 415–420. doi:10.1016/j.aspen.2021.01.005
- Scaloni, A., Monti, M., Angeli, S., and Pelosi, P. (1999). Structural analysis and disulfide-bridge pairing of two odorant-binding proteins from *Bombyx mori*. *Biochem. Biophys. Res. Co.* 266 (2), 386–391. doi:10.1006/bbrc.1999.1791
- Song, J. Y., Lee, G., Jung, J., Moon, J. K., and Kim, S. G. (2022). Effect of soybean volatiles on the behavior of the bean bug, *Riptortus pedestris*. *J. Chem. Ecol.* 48 (2), 207–218. doi:10.1007/s10886-021-01343-1
- Sparks, J. T., Bohbot, J. D., and Dickens, J. C. (2014). The genetics of chemoreception in the labella and tarsi of *Aedes aegypti*. *Insect biochem. molec.* 48 (1), 8–16. doi:10.1016/j.ibmb.2014.02.004
- Spinelli, S., Lagarde, A., Iovinella, I., Legrand, P., Tegoni, M., Pelosi, P., et al. (2012). Crystal structure of *Apis mellifera* OBP14, a C-minus odorant-binding protein, and its complexes with odorant molecules. *Insect biochem. molec.* 42 (1), 41–50. doi:10.1016/j.ibmb.2011.10.005
- Sun, Y. F., Qiao, H. L., Ling, Y., Yang, S. X., Rui, C. H., Pelosi, P., et al. (2011). New analogues of (E)- $\beta$ -farnesene with insecticidal activity and binding affinity to aphid odorant-binding proteins. *J. Agric. Food Chem.* 59 (6), 2456–2461. doi:10.1021/jf104712c
- Sun, Y. L., Huang, L. Q., Pelosi, P., and Wang, C. Z. (2012). Expression in antennae and reproductive organs suggests a dual role of an odorant-binding protein in two sibling *Helicoverpa* species. *PLoS ONE* 7 (1), e30040. doi:10.1371/journal.pone.0030040
- Tang, H. Y., Xie, J. X., Liu, J. T., Khashaveh, A., Liu, X. X., Yi, C. Q., et al. (2023). Odorant-binding protein HvarOBP5 in ladybird *Hippodamia variegata* regulates the perception of semiochemicals from preys and habitat plants. *J. Agric. Food Chem.* 71 (2), 1067–1076. doi:10.1021/acs.jafc.2c07355
- Trott, O., and Olson, A. J. (2010). AutoDock Vina: improving the speed and accuracy of docking with a new scoring function, efficient optimization, and multithreading. *J. Comput. Chem.* 31 (2), 455–461. doi:10.1002/jcc.21334
- Ullah, R. M. K., Quershi, S. R., Adeel, M. M., Abdelnabby, H., Waris, M. I., Duan, S. G., et al. (2020). An odorant binding protein (SaveOBP9) involved in chemoreception of the wheat aphid *Sitobion avenae*. *Int. J. Mol. Sci.* 21 (21), 8331. doi:10.3390/ijms21218331
- Ventur, H., Mutis, A., Zhou, J., and Quiroz, A. (2014). Ligand binding and homology modelling of insect odorant-binding proteins. *Physiol. Entomol.* 39 (3), 183–198. doi:10.1111/phen.12066
- Ventur, H., and Zhou, J. (2018). Odorant receptors and odorant-binding proteins as insect pest control targets: a comparative analysis. *Front. Physiol.* 9, 1163. doi:10.3389/fphys.2018.01163
- Vogt, R. G., and Riddiford, L. M. (1981). Pheromone binding and inactivation by moth antennae. *Nature* 293 (5828), 161–163. doi:10.1038/293161a0
- Wang, B., Dong, W. Y., Li, H. M., D'Onofrio, C., Bai, P. H., Chen, R. P., et al. (2022). Molecular basis of (E)- $\beta$ -farnesene-mediated aphid location in the predator *Eupeodes corolla*. *Curr. Biol.* 32 (5), 951–962.e7. doi:10.1016/j.cub.2021.12.054
- Wang, J. Z., Peng, G., Luo, Y. Q., and Tao, J. (2019). Characterization and expression profiling of odorant-binding proteins in *Anoplophora glabripennis* Motsch. *Gene* 693 (1), 25–36. doi:10.1016/j.gene.2018.12.075
- Wang, L., Bi, Y. D., Liu, M., Li, W., Liu, M., Di, S. F., et al. (2019). Identification and expression profiles analysis of odorant-binding proteins in soybean aphid, *Aphis glycines* (Hemiptera: aphididae). *Insect Sci.* 27 (5), 1019–1030. doi:10.1111/1744-7917.12709
- Wang, L. Y., Liu, Q. Y., Guo, P., Gao, Z. L., Chen, D., Zhang, T., et al. (2023). Evaluation of reference genes for quantitative real-time PCR analysis in the bean bug, *Riptortus pedestris* (Hemiptera: Alydidae). *Insects* 14 (12), 960–973. doi:10.3390/insects14120960
- Xiao, Y., Sun, L., Wu, Y. H., Wang, Q., Zhang, Y. J., Jing, X. F., et al. (2023). The larvae of *Phyllotreta striolata* share the same olfactory cues for locating Brassicaceae plant with conspecific adults. *J. Pest Sci.* 97 (2), 979–992. doi:10.1007/s10340-023-01690-w
- Yang, Y. T., Luo, L., Tian, L. X., Zhao, C. W., Niu, H. L., Hu, Y. F., et al. (2021). Function and characterization analysis of BodoOBP8 from *Bradysia odoriphaga* (Diptera: sciaridae) in the recognition of plant volatiles and sex pheromones. *Insects* 12 (10), 879–891. doi:10.3390/insects12100879
- Yasuda, T., Mizutani, N., Honda, Y., Endo, N., Yamaguchi, T., Moriya, S., et al. (2007). A supplemental component of aggregation attractant pheromone in the bean bug *Riptortus clavatus* (Thunberg) (Heteroptera: Alydidae), related to food exploitation. *Appl. Entomol. Zool.* 42 (1), 161–166. doi:10.1303/aer.2007.161
- Yin, M. Z., Li, J. Q., Liu, Q., Ma, S., Hu, Z. Z., Liu, X. Z., et al. (2023). Binding properties of chemosensory protein 12 in *Riptortus pedestris* to aggregation pheromone (E)-2-hexenyl (Z)-3-hexenoate. *Pestic. Biochem. Phys.* 194, 105513. doi:10.1016/j.pestbp.2023.105513
- Zeng, Y., Yang, Y. T., Wu, Q. J., Wang, S. L., Xie, W., and Zhang, Y. J. (2019). Genome-wide analysis of odorant-binding proteins and chemosensory proteins in the sweet potato whitefly, *Bemisia tabaci*. *Insect Sci.* 26 (4), 620–634. doi:10.1111/1744-7917.12576
- Zhang, F. M., Merchant, A., Zhao, Z. B., Zhang, Y. H., Zhang, J., Zhang, Q. W., et al. (2020). Characterization of MaltOBP1, a minus-c odorant-binding protein, from the Japanese pine sawyer beetle, *Monochamus alternatus* Hope (Coleoptera: cerambycidae). *Front. Physiol.* 11, 212. doi:10.3389/fphys.2020.00212
- Zhang, J., Luo, D., Wu, P., Li, H. Z., Zhang, H. Y., and Zheng, W. W. (2018). Identification and expression profiles of novel odorant binding proteins and functional analysis of OBP99a in *Bactrocera dorsalis*. *Arch. Insect Biochem.* 98 (1), e21452. doi:10.1002/arch.21452
- Zhang, Q. H., Schneidmiller, R., and Hoover, D. (2013). Essential oils and their compositions as spatial repellents for pestiferous social wasps. *Pest Manag. Sci.* 69 (4), 542–552. doi:10.1002/ps.3411
- Zhang, Q. H., Schneidmiller, R. G., Hoover, D. R., Zhou, G. J., Margaryan, A., and Bryant, P. (2014). Essential oils as spatial repellents for the brown marmorated stink bug, *Halyomorpha halys* (Stål) (Hemiptera: pentatomidae). *J. Appl. Entomol.* 138 (7), 490–499. doi:10.1111/jen.12101
- Zhang, Q. K., Li, Z. B., Chen, D. K., Wu, S. Y., Wang, H. H., Li, Y. L., et al. (2022). The molecular identification, odor binding characterization, and immunolocalization of odorant-binding proteins in *Liriomyza trifolii*. *Pestic. Biochem. Phys.* 181 (6), 105016. doi:10.1016/j.pestbp.2021.105016
- Zhang, X., Huang, C., Wu, Q., Yang, N. W., Qian, W. Q., and Wan, F. H. (2021). Advances in the study of general odorant binding proteins in insects. *J. Biosaf.* 30 (1), 11–19. doi:10.3969/j.issn.2095-1787.2021.01.003
- Zhang, X. Q., Yan, Q., Li, L. L., Xu, J. W., Mang, D. Z., Wang, X. L., et al. (2020). Different binding properties of two general-odorant binding proteins in *Aethis lepigone* with sex pheromones, host plant volatiles and insecticides. *Pestic. Biochem. Phys.* 164, 173–182. doi:10.1016/j.pestbp.2020.01.012
- Zheng, W., Zhang, C. X., Li, Y., Pearce, R., Bell, E. W., and Zhang, Y. (2021). Folding non-homologous proteins by coupling deep-learning contact maps with I-TASSER assembly simulations. *Cell Rep. Methods* 1, 100014. doi:10.1016/j.crmeth.2021.100014
- Zhou, J. J., Field, L., and He, X. L. (2010). Insect odorant-binding proteins: do they offer an alternative pest control strategy? *Outlooks Pest Manag.* 21 (1), 31–34. doi:10.1564/21feb08
- Zhou, X., Wang, Z., Cui, G. C., Du, Z. M., Qian, Y. L., Yang, S. M., et al. (2022). Binding properties of odorant-binding protein 4 of *Tirathaba rufivena* to areca catechu volatiles. *Plants* 11 (2), 167–178. doi:10.3390/plants11020167
- Zhu, J., Zaremska, V., D'Onofrio, C., Knoll, W., and Pelosi, P. (2020). Site-directed mutagenesis of odorant-binding proteins. *Method. Enzymol.* 642, 301–324. doi:10.1016/b.s.mie.2020.05.014
- Zhu, J. Q., Wang, F., Zhang, Y. J., Yang, Y. T., and Hua, D. K. (2023). Odorant-binding protein 10 from *Bradysia odoriphaga* (Diptera: sciaridae) binds volatile host plant compounds. *J. Insect Sci.* 23 (1), 7–8. doi:10.1093/jisesa/iead004
- Zhu, X. Y., Li, J. B., Liu, L., Dewar, Y., Zhang, H., Zhang, H. R., et al. (2022). Binding properties of odorant-binding protein 4 from bean bug *Riptortus pedestris* to soybean volatiles. *Insect Mol. Biol.* 31 (6), 760–771. doi:10.1111/imb.12802
- Zhuang, X., Wang, Q., Wang, B., Zhong, T., Cao, Y., Li, K. B., et al. (2014). Prediction of the key binding site of odorant-binding protein of *Holotrichia oblitata* Faldermann (Coleoptera: scarabaeida). *Insect Mol. Biol.* 23 (3), 381–390. doi:10.1111/imb.12088